Luminescence Polarization Spectroscopy Study of Functionalized Carbon Nanotubes in a Polymeric Matrix

Bing Zhou, Yi Lin, L. Monica Veca, K. A. Shiral Fernando, Barbara A. Harruff, and Ya-Ping Sun*

Department of Chemistry and Laboratory for Emerging Materials and Technology, Clemson University, Clemson, South Carolina 29634-0973

Received: September 27, 2005; In Final Form: December 8, 2005

Single-walled carbon nanotubes (SWNTs) were well-functionalized for a study of their defect-derived luminescence properties. The soluble nanotube sample was homogeneously dispersed in poly(vinyl alcohol) (PVA) films via solution-phase mixing and then wet-casting. The PVA films embedded with the functionalized SWNTs were strongly luminescent according to spectroscopic and confocal microscopic results. The luminescence from the films was highly polarized, with the observed anisotropy value approaching the limit for collinear absorption and emission dipole moments. The films were mechanically stretched to align the embedded nanotubes, and results from luminescence measurements of the stretched films suggested that the excitation was strongly in favor of the direction along the nanotube axis. Mechanistic implications of the polarization spectroscopy results for the luminescent functionalized nanotubes in the polymeric matrix with and without the mechanic alignment are discussed.

Introduction

The electronic structures and transitions and related optical absorption and emission properties of carbon nanotubes have been attracting much attention.[1−4] For single-walled carbon nanotubes (SWNTs), the optical absorption is characterized by spectral features in the near-IR, corresponding to electronic transitions associated with the van Hove singularity pairs in the electronic density of states.[1,2] It has been reported that under well-controlled experimental conditions semiconducting SWNTs exhibit characteristic band-gap fluorescence.[4,5] These required conditions include the individual nanotube dispersion, often assisted by the use of surfactants to form micelles, and minimal nanotube surface doping effects and/or defects.[5−8] The band-gap fluorescence of semiconducting SWNTs is generally weak, with quantum yields estimated to be on the order of 0.001.[4,5,9]

Most carbon nanotubes have surface defects, especially with the fact that surface defects may be produced in the widely employed effective purification procedures (such as oxidative acid treatment).[10,11] These defects have been exploited as sites for covalent functionalization of carbon nanotubes for their dispersion and solubilization. It has been shown that the well-functionalized carbon nanotubes are strongly luminescent, with quantum yields higher than 10% under some conditions, and the observed emission spectra cover a broad visible wavelength region and extend well into the near-IR.[12−16] The strong luminescence often represents overwhelming interference in Raman measurements of functionalized carbon nanotubes, in particular when the functionalization is effective, and as a result the nanotubes are individually dispersed.[16,17] Mechanistically, the surface defects upon passivation in the functionalization may serve as excitation energy traps to be responsible for the strong luminescence.[12−16] In fact, the need for functionalization and the dependence of observed luminescence intensities on how well the nanotube surface defects are passivated via the functionalization have recently been demonstrated.[16] As in band-gap fluorescence,[4,5] the defect-derived luminescence is also sensitive to the intertube quenching in nanotube bundles, and thus the effective exfoliation to obtain individually dispersed nanotubes is required for the observation of high luminescence intensities.[16]

The luminescence from functionalized carbon nanotubes in solution is somewhat polarized,[13] suggesting the presence of correlation between the electronic transitions associated with absorption and emission. Since SWNTs with the one-dimensional structure are intrinsically anisotropic, their alignment in an anisotropic polymeric host provides an opportunity to study the anisotropic nature of their electronic structures and transitions. Of particular interest is the orientation of the electronic absorption that corresponds to the observed strong luminescence in functionalized nanotubes. In optical spectroscopic investigations, stretched poly(vinyl alcohol) (PVA) films are widely employed as anisotropic polymeric hosts for the alignment of linear molecular chromophores,[18] including carbon nanotubes.[19]

In the work reported here, we dispersed well-functionalized SWNTs into PVA films, which thus became strongly luminescent, with the observed anisotropy value approaching the limit for collinear absorption and emission dipole moments. The films were mechanically stretched to align the embedded nanotubes, and luminescence measurements were employed to evaluate the polarization of optical absorption with respect to the alignment. The results suggest that the strong luminescence is indeed associated with the excited states of functionalized carbon nanotubes and is polarized along the nanotube axis. There is also a valuable bonus from the reported investigation, namely, that luminescence polarization can be used as an effective and very sensitive tool in the evaluation of nanotube alignment in polymeric nanocomposites, especially those of high quality in which the carbon nanotubes are homogeneously dispersed.

Experimental Section

Materials. 1,6-Diphenyl-1,3,5-hexatriene (DPH), poly(propionylethylenimine) (PPEI, $M_W \approx 200\,000$ kDa), and poly(vinyl

10.1021/jp055501r CCC: $33.50
Published on Web 01/31/2006

alcohol) (PVA, $M_W \approx 70\,000-100\,000$ kDa, 98−99% hydrolyzed) were purchased from Aldrich. Arc-discharge SWNT samples were either purchased from Carbon Solutions Inc. or produced in the laboratory of Professor A. M. Rao (Department of Physics, Clemson University). The as-received samples were purified according to established procedures (the nitric acid treatment),[10,20] including the additional use of cross-flow filtration in some purification experiments.[11,21] No fundamental difference was found in the spectroscopic results with respect to the different sample sources and variations in the sample purification.

PPEI-EI−SWNT. Poly(propionylethylenimine-*co*-ethylenimine) (PPEI-EI) was prepared by partially hydrolyzing PPEI in an acid-catalyzed reaction. Details on the reaction and product characterization are already available in the literature.[22,23]

The functionalization of SWNTs with PPEI-EI was based on the acylation−amidation of the nanotube-bound carboxylic acid moieties, similar to what was reported earlier.[12,22] Briefly, a purified SWNT sample (20 mg) was refluxed with thionyl chloride (5 mL) for 24 h, followed by evaporation to remove the excess thionyl chloride. To the treated nanotube sample was added carefully dried PPEI-EI (200 mg), and the mixture was heated to ∼170 °C. After the reaction for 12 h under nitrogen protection, the mixture was cooled to room temperature. To the mixture was added chloroform, followed by brief sonication and then centrifugation (3000*g*) to retain the colored supernatant. The procedure of extraction with chloroform was repeated multiple times, and the soluble fractions were combined, concentrated, and precipitated into hexane. The PPEI-EI-functionalized SWNT (PPEI-EI−SWNT) sample was obtained as a dark-colored solid. The sample was characterized by a series of instrumental methods, as already reported in the literature.[20,24] According to the thermogravimetric analysis, the nanotube content in the PPEI-EI−SWNT sample used in this study was ∼10% (wt/wt).

PVA Films. A concentrated aqueous solution of PVA was prepared by dissolving PVA (2 g) in deionized water (10 mL) at 80 °C with vigorous stirring. Upon being cooled to ambient temperature, the solution was stirred slowly for up to 12 h for the removal of air bubbles. To the PVA solution was added dropwise an aqueous solution of PPEI-EI−SWNT (4 mg/mL, 5 mL) with constant stirring. The resulting mixture was stirred for another 4 h to obtain a viscous and colored solution without visible aggregates or air bubbles. The solution was poured onto a glass slide for film casting by using an adjustable film applicator (from Gardco). The supported film was placed in a dust-free environment at room temperature with continuous air flow for 24 h and then at 60 °C under vacuum for 48 h. The film (100−150 μm in thickness) could be peeled off the glass substrate to be free-standing. It was cut into 2 cm × 3 cm strips for mechanical stretching. In a typical stretching experiment, a film strip was mounted on a homemade manual stretching frame and heated to ∼110 °C (above the T_g of PVA ≈ 85 °C). A constant load was applied to both ends of the strip for stretching until the desired draw ratio (the length after stretching/the initial length), followed by cooling to room temperature.

Measurements. Optical absorption spectra were recorded on Shimadzu UV2101PC and UV3100 spectrophotometers and a Thermo-Nicolet Nexus 670 FT-NIR spectrometer. Luminescence emission spectra were measured on a Spex Fluorolog-2 emission spectrometer equipped with a 450 W xenon source, a Spex 340S dual-grating and dual-exit emission monochromator, and two detectors. The two gratings are blazed at 500 nm (1200 grooves/mm) and 1000 nm (600 grooves/mm). The room-temperature detector consists of a Hamamatsu R928P photomultiplier tube operated at 950 V, and the thermoelectrically cooled detector consists of a near-IR sensitive Hamamatsu R5108 photomultiplier tube operated at 1500 V. Unless specified otherwise, the reported spectra were corrected for nonlinear instrumental response by use of predetermined emission correction factors.

Two Melles-Griot dichroic sheet polarizers were used in a right-angle geometry in the luminescence emission measurements for the determination of luminescence anisotropy r[18]

$$P = (I_{HH}I_{VV} - I_{HV}I_{VH})/(I_{HH}I_{VV} + I_{HV}I_{VH}) \quad (1)$$

$$r = 2P/(3 - P) \quad (2)$$

where the indices V and H denote the vertical and horizontal positions of the polarizers, respectively, in the excitation and emission beam paths. The theoretical range of r is from −0.2 (absorption and emission transition dipoles perpendicular) to 0.4 (the two dipoles collinear).[18]

Confocal microscopy images were obtained on a Carl-Zeiss LSM510 laser scanning confocal fluorescence microscope equipped with an argon ion laser and a HeNe laser for excitation at multiple wavelengths. The oil immersion corrected objective lens allows magnifications up to 63 times (large numeric aperture number 1.3). The typical pinhole size for plane mode imaging was 150 μm.

Results

DPH-in-PVA Film. DPH was dispersed in a PVA film via solution mixing and then casting. The free-standing film was of high optical transparency, and the UV/vis absorption spectrum of DPH in the film was similar to that in the solution phase. At 370 nm excitation for the film, the observed fluorescence anisotropy r is 0.39, in excellent agreement with the literature results.[25,26]

The free-standing PVA film embedded with DPH was mechanically stretched to a draw ratio of 5. With a linear polarizer at the excitation slit in the emission spectrometer, the observed fluorescence spectra were strongly dependent on the relative orientation of the stretched film with respect to the polarization direction, exhibiting much higher intensities when the two were parallel. To take into consideration the nonlinear instrument response to the polarized light, the film before stretching was measured under the same experimental conditions to use the results as references. The average dichroic ratio (emission wavelengths 400−550 nm) with the correction for nonlinear instrument response was 13.6, again in excellent agreement with the results already in the literature.[18]

Functionalized SWNTs in PVA Film, No Stretching. Similar to the DPH-in-PVA film discussed above, the free-standing PVA films embedded with PPEI-EI−SWNT appeared homogeneous, with equally high optical quality (Figure 1). The optical absorption spectrum of the film with a relatively low PPEI-EI−SWNT loading is a featureless curve (Figure 2). However, at a higher nanotube loading in the film and/or with increased film thickness, the optical absorption spectra of PPEI-EI−SWNT in a PVA matrix exhibit the characteristic S_{11} and S_{22} bands in the near-IR, similar to those of purified SWNTs dispersed in a PVA film (Figure 2, inset).

Even at a low optical density, the PVA film embedded with PPEI-EI−SWNT is strongly luminescent, with the spectra generally similar to those in solution at the same excitation

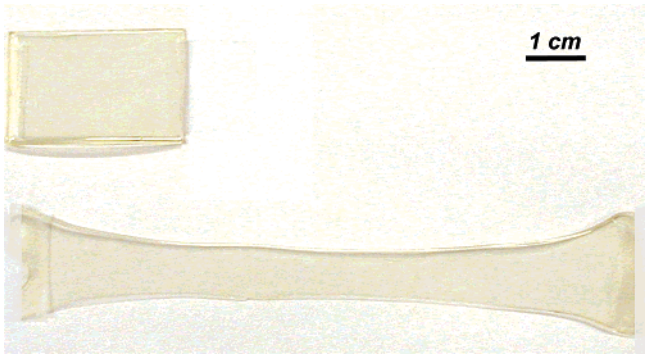

Figure 1. PVA films embedded with PPEI-EI−SWNT: as-prepared (top) and stretched to a draw ratio of 5 (bottom).

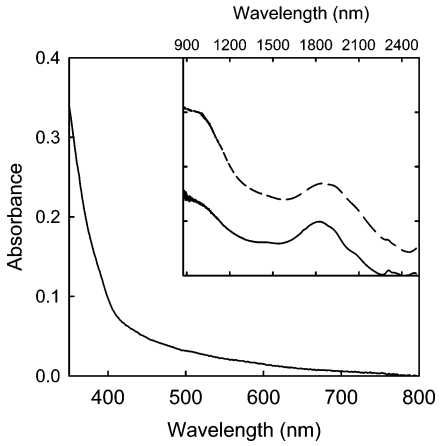

Figure 2. UV/vis absorption spectrum of PPEI-EI−SWNT in PVA film (the nanotube content on the order of 0.1 wt %/wt). Compared in the inset are the absorption spectra in near-IR for the same sample at a higher nanotube content (on the order of 2 wt %/wt, —) and purified SWNTs in PVA film (− − −).

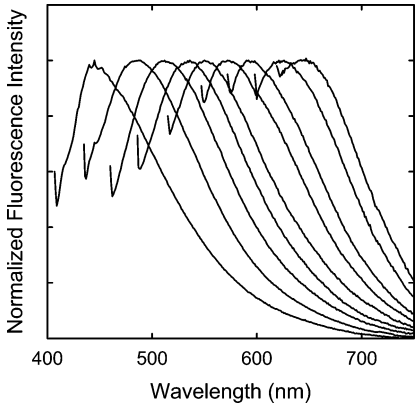

Figure 3. Luminescence emission spectra (normalized) of PPEI-EI−SWNT in PVA film with progressively longer excitation wavelengths of 400, 425, 450, 475, 500, 525, 550, 575, and 600 nm.

wavelengths. As shown in Figure 3, the observed emission spectra are dependent on the excitation in a similarly progressive fashion.[16]

The PVA film with PPEI-EI−SWNT was examined under a confocal microscope. Bright and homogeneous luminescence images (spatial resolution $\approx$ 0.5 μm) across the film were obtained. The confocal images at different depths beneath the film surface were examined to ensure their representation of the whole film matrix and to avoid any surface effects. Several available excitation wavelengths from 458 to 633 nm were used with respective long-pass emission filters on the confocal microscope, which all resulted in bright fluorescence images (Figure 4). The observed emission intensity expressed by the color intensity is generally uniform across the film, suggesting a good dispersion of the functionalized SWNTs in the PVA matrix and the absence of any microscopic phase separation.

Luminescence polarization measurement of PPEI-EI−SWNT in PVA film was carried out with two polarizers (one for excitation and the other for emission) in a right-angle geometry. The spectra were found to be strongly polarized. The anisotropy value (eq 2) for the excitation at 400 nm is 0.33, and it is generally independent of the emission wavelength (Figure 5). However, the polarization is somewhat dependent on the excitation wavelength (Table 1), larger at a longer excitation wavelength (0.39 for the excitation at 550 nm, Figure 5).

Functionalized SWNTs in PVA Film, Stretched. The PVA film embedded with PPEI-EI−SWNT was mechanically stretched to a draw ratio of up to 5, which was accompanied by a narrowing and thinning of the film (Figure 1). However, the nanotubes remained well-dispersed according to confocal microscopy images of the stretched films (Figure 6). These images also suggest that there is a preferential orientation of the functionalized nanotubes in the stretching direction. With the use of only one polarizer at the excitation slit, luminescence spectra of the stretched film corresponding to the polarizer being parallel and perpendicular to the stretching direction were measured. The nonlinear instrument responses in the two orientations were corrected by using a film of similar thickness but without the stretching (the same as the correction for the DPH-in-PVA film discussed above). The corrected luminescence emission intensities are obviously higher in the parallel direction than those in the perpendicular direction (Figure 7). The observed dichroic ratio is somewhat dependent on the excitation wavelength (Figure 7, inset).

The alignment of the functionalized SWNTs in the stretched PVA film was also evaluated in terms of the dependence of the observed dichroic ratio on the draw ratio. The excitation was at 500 nm, and the emission intensities obtained with the polarizer parallel and perpendicular to the stretching direction (after corrections in reference to the results of the unstretched film) were used to calculate the dichroic ratio. As shown in Figure 8 for the stretching with the film draw ratio from 1 to 7, the dichroic ratio initially increases rapidly with the increasing draw ratio and then reaches almost a plateau. Further stretching of the film to a draw ratio beyond 7 always resulted in the fracture of the film.

Discussion

The possibility of technical issues in experimental measurements of luminescence polarization was considered by using DPH as a calibration standard to evaluate the emission spectrometer, the measurement methods, and the sample preparation. DPH is a rodlike molecule, with the absorption and emission transition moments along the long molecular axis.[26] For DPH-in-PVA film at 370 nm excitation, the observed anisotropy value of 0.39 is in excellent agreement with what is known in the literature,[18,25] thus validating the experimental setup and methods.

Unlike in the determination of anisotropy in terms of eqs 1 and 2, corrections for the internal polarization of the spectrometer (such as different sensitivities of gratings and the detection toward light at different polarization angles) are required in the measurement of stretched film with only one polarizer at the excitation slit. Experimentally, unstretched films of similar optical densities to those of the stretched films were measured

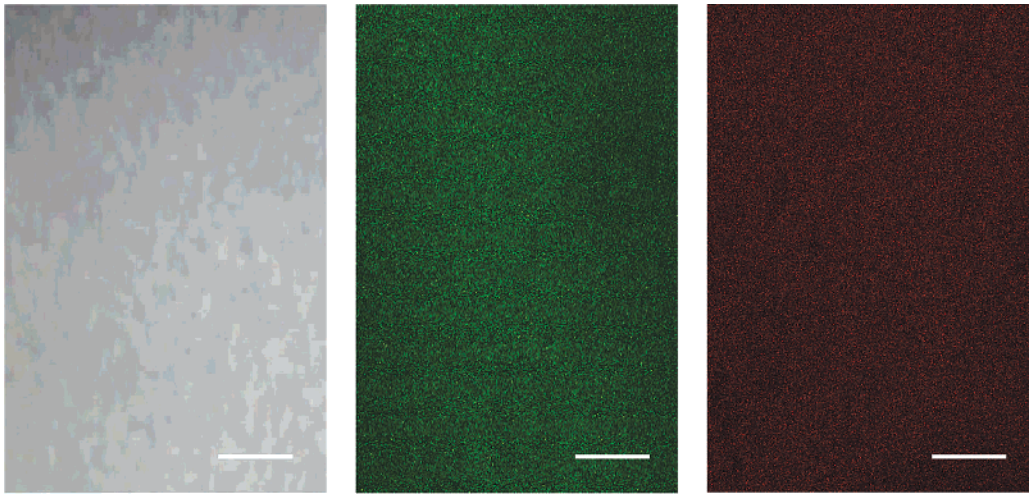

Figure 4. Optical (left) and confocal microscopy images (middle, 514 nm excitation, >530 nm detection; right, 633 nm excitation, >650 nm detection) of a PVA film embedded with PPEI-EI−SWNT (20 μm for all scale bars).

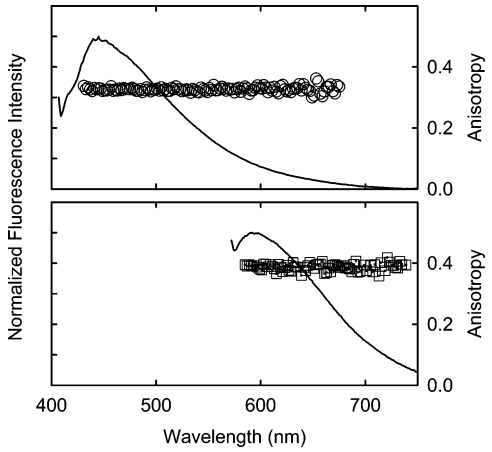

Figure 5. Luminescence emission spectra and corresponding anisotropy values of PPEI-EI−SWNT in PVA film with the excitation at 400 nm (top) and 550 nm (bottom).

TABLE 1: Luminescence Anisotropy (*r*) Values at Different Excitation Wavelengths

excitation wavelength (nm)	400	425	450	475	500	525	550	575	600
$r_{solution}$[a]	0.052	0.069	0.10	0.12	0.14	0.15	0.16	0.18	0.19
r_{film}	0.32	0.34	0.35	0.35	0.37	0.38	0.39	0.39	0.39

[a] From repeating the experiments reported in ref 13.

in the same instrument configuration to estimate the required corrections. It was found that the spectrometer used in this study is relatively uniform at different polarization angles, with the corrections generally less than 10%. For DPH in the stretched PVA film, the agreement between the dichroic ratio obtained in this study and the literature value is excellent.[18]

The exfoliation of bundled SWNTs was achieved via covalent functionalization with the aminopolymer PPEI-EI, where the nanotube surface defects were targeted for the formation of amide linkages.[12,17] In PPEI-EI−SWNT, the dispersion of the nanotubes and the passivation of surface defects are known to be especially effective, resulting in relatively strong visible luminescence. However, the covalent functionalization has little effect on the electronic transitions associated with the van Hove singularity pairs in semiconducting SWNTs,[16,21] with the S_{11} and S_{22} absorption features in the near-IR largely unchanged before and after the functionalization (Figure 2).

The selection of PPEI-EI−SWNT in this study was also due to their solubility in water; thus they are readily miscible with an aqueous solution of PVA to allow the fabrication of nanocomposite thin films via wet-casting.[21] The films were of high optical quality, exhibiting few scattering contributions in observed absorption and emission spectra. The microscopically homogeneous dispersion of nanotubes in the films was confirmed by the laser scanning confocal microscopy results for imaging at different depths of the film. The bright confocal images also allow a visual appreciation for the films being strongly luminescent (Figure 4).

The luminescence of the functionalized carbon nanotubes is obviously polarized in both solution and PVA thin film, namely, that the absorption and emission dipole moments are correlated despite the fact that the observed luminescence emission is likely associated with excited state energy trapping by well-passivated nanotube surface defects. This and the excitation wavelength dependence of luminescence properties seem to suggest that the excitation is at least partially localized in a distribution of electronic states in the functionalized carbon nanotubes. The anisotropy values in PVA thin films are clearly larger than those in solution (Table 1), which may be attributed to the restriction to any movement (and reorientation depolarization) of the nanotubes in the more rigid polymeric matrix. In particular, the excitation wavelength dependence of the anisotropy becomes less significant in the films (Table 1), with the limiting anisotropy value of 0.4 reached at longer excitation wavelengths. The results may be interpreted as such that there is probably somewhat more energy migration associated with excitation into higher energy states, but the depolarization effect is relatively insignificant. The absorption and emission dipole moments are close to being parallel for the functionalized carbon nanotubes dispersed in the polymeric matrix. However, the luminescence anisotropy results provide no information on the orientation of these parallel dipoles with respect to the nanotube structure. Experiments with the nanotubes aligned in stretched PVA films are required to address the issue.

The measurement of luminescence emissions from the stretched films is a more sensitive alternative to the direct determination of absorption polarization in reference to the film stretching direction. It has been established that the mechanical stretching of PVA film results in a significant alignment of the embedded SWNTs,[19] similar to the alignment of DPH in the same matrix discussed above. Thus, the observed dichroic ratio strongly in favor of the film stretching direction (Figure 7)

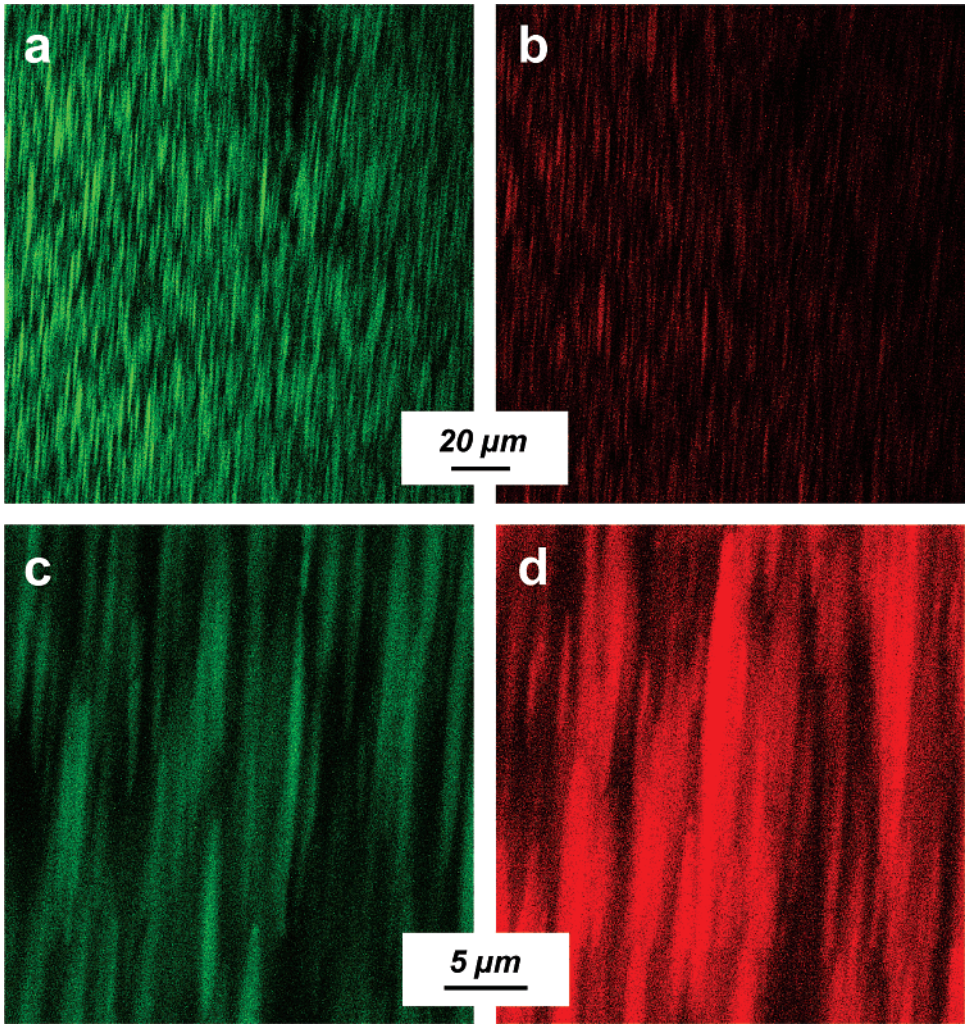

Figure 6. Confocal microscopy images of PPEI-EI−SWNT in PVA film after mechanical stretching to a draw ratio of about 5 (a and c, 514 nm excitation, >530 nm detection; b and d, 633 nm excitation, >650 nm detection).

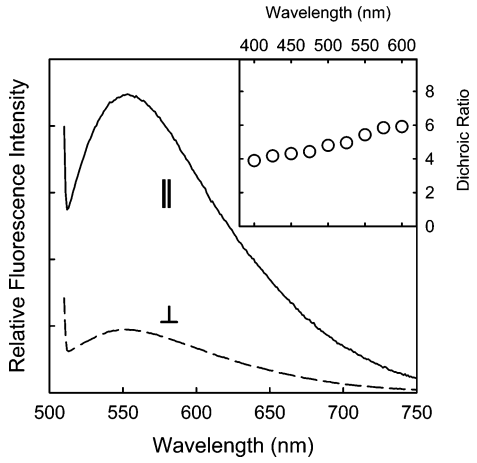

Figure 7. Luminescence emission spectra of PPEI-EI−SWNT in stretched PVA film (draw ratio ≈ 5) excited with polarized light parallel (||, —) and perpendicular (⊥, — — —) to the stretching direction. Shown in the inset is the excitation wavelength dependence of the observed dichroic ratio.

indicates that the electronic absorption responsible for the luminescence properties is along the nanotube long axis. When this is combined with the luminescence anisotropy results, an obvious conclusion is that both the absorption and emission dipole moments are coaxial with the functionalized carbon nanotubes.

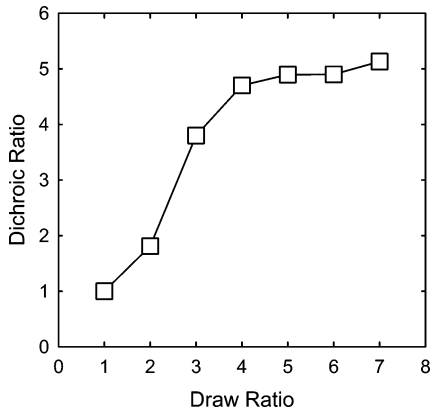

Figure 8. Observed dichroic ratio for PPEI-EI−SWNT in stretched PVA film as a function of the draw ratio (500 nm excitation).

Luminescence polarization spectroscopy apparently represents an effective tool in the evaluation of nanotube alignment in polymeric nanocomposites. For the functionalized SWNTs in the PVA film, the increasing dichroic ratio with the degree of stretching reflects the improvement in the nanotube alignment. The observed plateau in Figure 8 might be rationalized by the limitation or saturation in the use of stretched PVA film to create sufficient shear at large draw ratios. Separately, in the mechanical film stretching, the draw ratio for plain PVA films was generally limited to about 5 before the fracture of the films.[27]

For the PVA films embedded with PPEI-EI−SWNTs, however, a larger draw ratio up to 7 could be achieved. This might be explained as the effect of reinforcement associated with the homogeneously dispersed SWNTs, despite the relatively low nanotube content (on the order of 0.1 wt %).

According to the calculation by Ajiki et al.,[28] the optical absorption in the direction parallel to the nanotube axis is up to 20 times larger than the absorption in the perpendicular direction. The observed dichroic ratio is obviously significantly smaller than such a computational prediction. One might argue that the nanotube alignment in the stretched PVA film is still far from being optimal, thus the extremely high nanotube aspect ratio is not adequately reflected in the luminescence polarization results. However, the average persistence length in the structure of carbon nanotubes with respect to electronic absorption and emission should also be considered. This is particularly significant to the defect-derived luminescence emission, which by nature should correspond to limited persistence length. Therefore, it is probably desirable in further investigations to compare the dichroic ratios obtained from the luminescence emission experiments with those determined from direct polarized absorption measurements, though the latter might involve considerable technical difficulties. Also deserving attention in further investigations is the observed dependence of the dichroic ratio on the excitation wavelength (Figure 7), for which there are many mechanistic possibilities.

Summary and Conclusion

Carbon nanotubes were well-functionalized with PPEI-EI polymer to result in strong defect-derived luminescence. The functionalized nanotubes could be homogeneously dispersed into PVA polymer matrix to obtain equally luminescent films. The observed luminescence in the films was found to be strongly polarized to the limit for collinear absorption and emission dipole moments. The PVA films were mechanically stretched to align the embedded carbon nanotubes. The evaluation of the stretched films by polarized luminescence excitation suggested that the optical absorption responsible for the luminescence emissions was polarized along the nanotube axis. Thus, the reported results reaffirm the previous conclusion that the strong luminescence from well-functionalized and well-dispersed carbon nanotubes must be associated with the electronic excited states of the nanotubes and reveal the fact that the optical absorption and the defect-derived luminescence emission are not only strongly correlated but also both collinear with the nanotube axis. The luminescence and polarization properties of functionalized carbon nanotubes may find valuable applications, such as the probing of nanotube alignment in nanocomposites and other systems.

Acknowledgment. We thank R. B. Martin, W. Huang and K. Fu for experimental assistance and Professor. A. M. Rao for supplying a nanotube sample. Financial support from the National Science Foundation, NASA, and the Center for Advanced Engineering Fibers and Films (NSF-ERC at Clemson University) is gratefully acknowledged.

References and Notes

(1) Jorio, A.; Saito, R.; Hertel, T.; Weisman, R. B.; Dresselhaus, G.; Dresselhaus, M. S. *MRS Bull.* **2004**, *29*, 276−280.

(2) Kataura, H.; Kumasawa, Y.; Maniwa, Y.; Umezu, I.; Suzuki, S.; Ohtsuka, Y.; Achiba, Y. *Synth. Met.* **1999**, *103*, 2555−2558.

(3) Sun, Y.-P.; Riggs, J. E.; Henbest, K. B.; Martin, R. B. *J. Nonlinear Opt. Phys. Mater.* **2000**, *9*, 481−503.

(4) (a) O'Connell, M. J.; Bachilo, S. M.; Huffman, C. B.; Moore, V. C.; Strano, M. S.; Haroz, E. H.; Rialon, K. L.; Boul, P. J.; Noon, W. H.; Kittrell, C.; Ma, J.; Hauge, R. H.; Weisman, R. B.; Smalley, R. E. *Science* **2002**, *297*, 593−596. (b) Bachilo, S. M.; Strano, M. S.; Kittrell, C.; Hauge, R. H.; Smalley, R. E.; Weisman, R. B. *Science* **2002**, *298*, 2361−2366.

(5) (a) Lebedkin, S.; Hennrich, F.; Skipa, T.; Kappes, M. M. *J. Phys. Chem. B* **2003**, *107*, 1949−1956. (b) Lebedkin, S.; Arnold, K.; Hennrich, F.; Krupke, R.; Renker, B.; Kappes, M. M. *New J. Phys.* **2003**, *5*, 140.1−140.11.

(6) O'Connell, M. J.; Eibergen, E. E.; Doorn, S. K. *Nat. Mater.* **2005**, *4*, 412−418.

(7) Qin, S.; Qin, D.; Ford, W. T.; Herrera, J. E.; Resasco, D. E.; Bachilo, S. M.; Weisman, R. B. *Macromolecules* **2004**, *37*, 3965−3967.

(8) Lauret, J.-S.; Voisin, C.; Cassabois, G.; Roussignol, P.; Delalande, C.; Filoramo, A.; Capes, L.; Valentin, E.; Jost, O. *Physica E* **2004**, *21*, 1057−1060.

(9) Jones, M.; Engtrakul, C.; Metzger, W. K.; Ellingson, R. J.; Nozik, A. J.; Heben, M. J.; Rumbles, G. P. *Phys. Rev. B* **2005**, *71*, 115426.

(10) Haddon, R. C.; Sippel, J.; Rinzler, A. G.; Papadimitrakopoulos, F. *MRS Bull.* **2004**, *29*, 252−259.

(11) Liu, J.; Rinzler, A. G.; Dai, H.; Hafner, J. H.; Bradley, R. K.; Boul, P. J.; Lu, A.; Iverson, T.; Shelimov, K.; Huffman, C. B.; Rodriguez-Macias, F.; Shon, Y. S.; Lee, T. R.; Colbert, D. T.; Smalley, R. E. *Science* **1998**, *280*, 1253−1256.

(12) Riggs, J. E.; Guo, Z.; Carroll, D. L.; Sun, Y.-P. *J. Am. Chem. Soc.* **2000**, *122*, 5879−5880.

(13) Sun, Y.-P.; Zhou, B.; Henbest, K.; Fu, K.; Huang, W.; Lin, Y.; Taylor, S.; Carroll, D. L. *Chem. Phys. Lett.* **2002**, *351*, 349−353.

(14) Guldi, D. M.; Holzinger, M.; Hirsch, A.; Georgakilas, V.; Prato, M. *Chem. Commun.* **2002**, 1130−1131.

(15) Banerjee, S.; Wong, S. S. *J. Am. Chem. Soc.* **2002**, *124*, 8940−8948.

(16) Lin, Y.; Zhou, B.; Martin, R. B.; Henbest, K. B.; Harruff, B. A.; Riggs, J. E.; Guo, Z. X.; Allard, L. F.; Sun Y.-P. *J. Phys. Chem B* **2005**, *109*, 14779−14782.

(17) Sun, Y.-P.; Fu, K.; Huang, W.; Lin, Y. *Acc. Chem. Res.* **2002**, *35*, 1096−1104.

(18) (a) Lakowicz, R. J. *Principles of Fluorescence Spectroscopy*, 2nd ed.; Kluwer Academic/Plenum Publisher: New York, 1999. (b) Michl, J.; Bonacic-Koutechý, V. *Electronic Aspects of Organic Photochemistry*; John Wiley & Sons: New York, 1990.

(19) Rozhin, A. G.; Sakakibara, Y.; Kataura, H.; Matsuzaki, S.; Ishida, K.; Achiba, Y.; Tokumoto, M. *Chem. Phys. Lett.* **2005**, *405*, 288−293.

(20) Lin, Y.; Hill, D. E.; Bentley, J.; Allard, L. F.; Sun, Y.-P. *J. Phys. Chem. B* **2003**, *107*, 10453−10457.

(21) Lin, Y.; Zhou, B.; Fernando, K. A. S.; Liu, P.; Allard, L. F.; Sun, Y.-P. *Macromolecules* **2003**, *36*, 7199−7204.

(22) Lin, Y.; Rao, A. M.; Sadanadan, B.; Kenik, E. A.; Sun, Y.-P. *J. Phys. Chem. B* **2002**, *106*, 1294−1298.

(23) Sun, Y.-P.; Liu, B.; Moton, D. K. *Chem. Commun.* **1996**, 2699−2700.

(24) Fernando, K. A. S.; Lin, Y.; Sun, Y.-P. *Langmuir* **2004**, *20*, 4777−4778.

(25) Patra, D. *J. Appl. Spectrosc.* **2004**, *71*, 334−338.

(26) Valeur, B. *Molecular Fluorescence: Principles and Applications*; Wiley-VCH Verlag GmbH: Weinheim, Germany, 2001.

(27) Dirix, Y.; Tervoort, T. A.; Bastiaansen, C. *Marcomolecules* **1997**, *30*, 2175−2177.

(28) (a) Ajiki, H.; Ando, T. *Physica B* **1994**, *201*, 349−352. (b) Duesberg, G. S.; Loa, I.; Burghard, M.; Syassen, K.; Roth, S. *Phys. Rev. Lett.* **2000**, *85*, 5436−5439.